

Topological Magnetic Heuslers

Satya N. Guin[#], Kaustuv Manna, Nitesh Kumar, Jonathan Noky, Chenguang Fu, Walter Schnelle, Chandra Shekhar, Yan Sun, Claudia Felser

The interplay between topology and magnetism has sparked interest in frontier studies of magnetic topological materials. We investigate the synthesis as well as magnetic, electrical, and thermal transport properties of various topological magnetic Heusler compounds, in addition to their electronic band structures, with angle-resolved photoemission spectroscopy experiments. We discovered a three-dimensional topological magnet, Co_2MnGa , for the first time. The material also exhibits one of the highest anomalous Hall conductivity, Nernst effect, and anomalous Hall angle among all magnetic Heuslers at room temperature. Moreover, we show symmetry and crystal-structure-based chemical design principles to choose layered magnets. In this study we investigate MnAlGe , a layered topological nodal-line magnet. The compound exhibits a unique 2D-Berry curvature distribution that results in a large anomalous Hall conductivity. Furthermore, we discuss our vision on anomalous transport for topological magnetic Heusler compounds. As a guiding tool, we use theoretically predicted Heusler candidates that show largely anomalous transport properties. In an initial successful experiment, we observed largely anomalous Hall and Nernst effects in Fe-based Heusler compounds, Fe_2YZ ($Y = \text{Co}, \text{Ni}$; $Z = \text{Al}, \text{Ga}$). In summary, our work helps in searching for new topological magnets and exploring their synthesis, magnetism, and topological properties.

Topological materials are a class of quantum materials wherein gapless electronic excitations are observed, which are protected by the crystal symmetry and topology of the bulk band structure. These materials have garnered tremendous attention in recent years due to their fascinating properties and potential for modern technological applications [1]. Magnetic Heusler compounds are a promising class of materials for this purpose because of the ease of tuning their structure, their magnetism, and their electronic structure that exhibits strong topological features.

In this study, we focus on understanding the electronic structure as well as electrical and thermoelectric properties of various topological magnetic Heuslers. Our investigation led to a deeper understanding of the tunability of transport properties in these systems which might result in the discovery of novel phenomena such as the quantum anomalous Hall effect at room temperature. We calculate the band structure and the Berry curvature distribution that acts as a guiding principle to understand the topological properties. The Berry curvature shows a strong effect in the case of protected band crossings in topological materials.

Discovery of first three-dimensional topological magnet Co_2MnGa

Evidence of topological state. Co_2MnGa is a full Heusler compound that crystallizes in the $L2_1$ structure with the space group $Fm\bar{3}m$ (Fig. 1a). It is found to be ferromagnetic with $T_C \sim 690$ K and a saturation magnetization value of $4 \mu_B \text{ f.u.}^{-1}$ at 2 K. A detailed

theoretical analysis of the band structure (Fig. 1b) of Co_2MnGa shows the formation of three nodal lines very close to E_F near the Γ point in the k_x , k_y , and k_z planes, and they are protected by the mirror symmetries M_x , M_y , and M_z . Motivated by these aspects, we investigated Co_2MnGa single crystals using angle-resolved photoemission spectroscopy (ARPES) and discovered the first three-dimensional topological magnetic phase. First, we successfully synthesized Co_2MnGa single crystals using the Bridgman method (Fig. 1c). A nodal line is formed

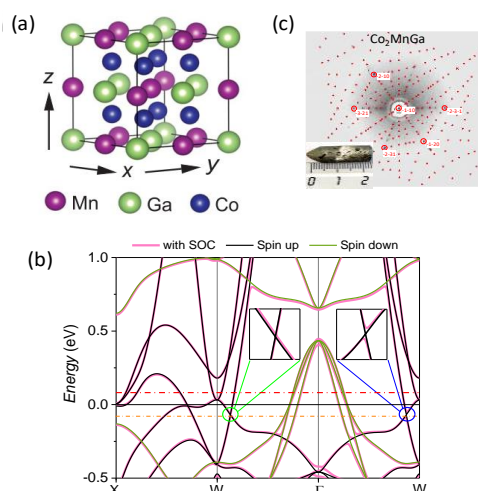


Fig. 1: (a) Crystal structure of Co_2MnGa ; (b) calculated band structure in Co_2MnGa with and without considering spin-orbit coupling (SOC). The band crossings are marked with the small circle and are zoomed in on the inset. SOC lifts the degeneracy and opens the crossing at the blue circle; (c) Bridgman-grown single crystal along with the Laue diffraction.

when two bands of opposite mirror eigenvalues cross (Fig. 2a). We observe a pair of bulk bands crossing along the curves in the bulk Brillouin zone, which are the topological line nodes associated with π Berry phase and protected by mirror symmetry. We plot the constant energy surfaces as a function of E_B . As we move from E_F to a deeper E_B value, we see that the line node feature changes from a ‘<’ shape to a ‘>’ shape (Fig. 2b-d), forming electron and hole pockets accordingly. For energies that cross the line node, we find electron and hole pockets intersecting at a point (Fig. 3h). All the line node features of the measured Fermi surface (Fig. 2e) match very well with the *ab initio* constant energy surface (Fig. 2f). To better understand this result, we consider E_B-k_x (k_x , in-plane crystal momentum) cuts passing through the node line feature (Fig. 2g). Considering a series of E_B-k_x ARPES cuttings at different k_y values, we located band crossing over a range of k_y , where E_B is the binding energy. The linear band crossing is the distinctive feature for observation of a line node and hence is different from the conventional Dirac or Weyl semimetals where crossing occurs at one particular k_y value. All of these results indicate the formation of topological line nodes in Co_2MnGa single crystals [2].

Colossal anomalous Hall effect in Co_2MnGa . After providing spectroscopic evidence for a magnetic bulk-boundary correspondence in Co_2MnGa , we investigate the relationship between the topological node lines and the anomalous Hall effect (AHE) [3]. Our experimental results show a strong Berry curvature from the nodal line-induced colossal anomalous Hall conductivity (AHC) of $\sim 1600 \text{ S cm}^{-1}$ at 2 K (Fig. 3a). We also observed a giant anomalous Hall angle (AHA) up to 12% at room temperature, which is the highest

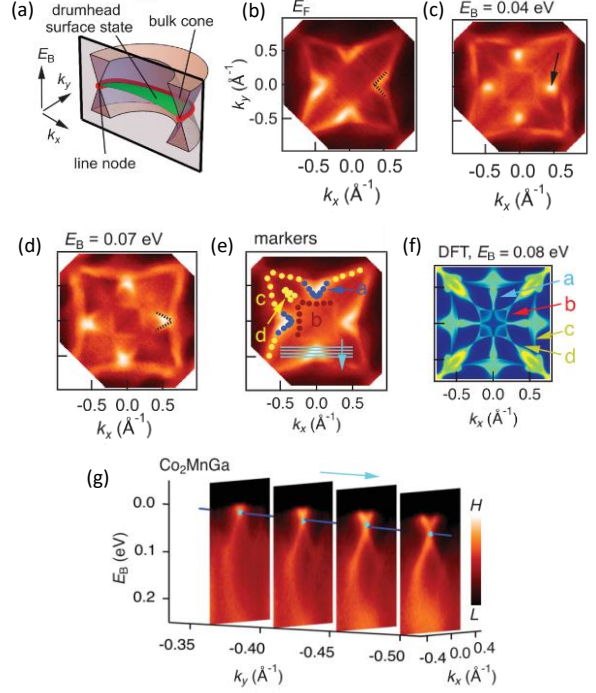


Fig. 2: (a) Schematic of a generic node line. A node line (red curve) is a band degeneracy along an entire curve in the bulk Brillouin zone (BZ). It is associated with a drumhead surface state stretching across the node line (green sheet). (b-d) Constant energy surfaces measured by ARPES at $h\nu = 50 \text{ eV}$ and $T = 20 \text{ K}$, presented at a series of binding energies, E_B , from the Fermi level, E_F , down to $E_B = 0.08 \text{ eV}$. (e) Key features of the data, obtained from analysis of the momentum and energy distribution curves of the ARPES spectra. (f) *Ab initio* constant-energy surface at binding energy $E_B = 0.08 \text{ eV}$ below E_F , on the (001) surface with MnGa termination, showing qualitative agreement with the ARPES, as marked by features a to d. (g) Series of ARPES E_B-k_x cuts through the candidate node line.

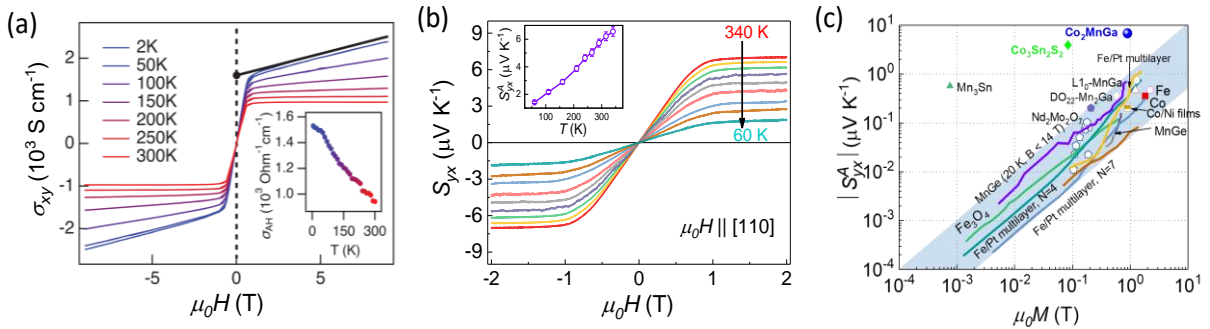


Fig. 3: (a) The Hall conductivity σ_{xy} , as a function of magnetic field μ_0H at different temperatures (T) in Co_2MnGa single crystals. The inset shows the T -dependent anomalous Hall conductivity. (b) Nernst thermopower (S_{yx}) at various T . The inset shows the T variation of the extracted anomalous Nernst thermopower (S_{yx}^A). (c) A comparison plot of the magnetization-dependent S_{yx}^A in various ferromagnetic metals. Co_2MnGa single crystals fall beyond magnetization scaling relation, as highlighted by the blue shaded region.

observed value in any magnetic Heusler reported so far in literature [2].

Anomalous Nernst effect in Co_2MnGa . The anomalous Nernst effect (ANE) is analogous to the electrical AHE, where a transverse voltage is generated perpendicular to both the heat flow and magnetization of the sample. For a long time, it was believed that the value of ANE is proportional to the net magnetic moment of the sample. However, recent investigation shows that the ANE originates from the net Berry curvature $[\Omega_n(\mathbf{k})]$ of all bands near E_F , and a large ANE can be observed beyond magnetization scaling [4]. We observed a remarkably high ANE value of $\sim 6.0 \mu\text{V K}^{-1}$ at 300 K (Fig. 3c) in Co_2MnGa single crystals. This is nearly a factor 7 larger than any anomalous Nernst thermopower value ever reported for any conventional ferromagnet (Fig. 3c). Combined electrical, thermoelectric, and first-principles calculations reveal that this high ANE value arises from a large net Berry curvature near the Fermi level associated with the nodal lines and Weyl points.

Layered topological magnet MnAlGe

Crystal and electronic structure. Following symmetry and crystal-structure-based chemical design principles is an important way to choose appropriate topological materials. Fig. 4a shows the evolution of tetragonal PbFCl, a ternary ordered variant of the Cu_2Sb -type structure (space group $P4/nmm$), by removing every second layer of atoms in the tetrahedral sites of the Cu_2MnAl -type ($Fm\bar{3}m$)

structure. Layered MnAlGe is a special example in this structure type with metallic character and ferromagnetism at a high Curie temperature ($T_C \sim 503$ K). Its ordered structure exhibits strongly anisotropic magnetism along the c -axis (i.e., the easy axis). The observed, ordered magnetic moment is $1.81 \mu_B$ per Mn atom. In the structure, the Mn atoms (denoted by blue spheres; Figure 1a) were formed in 4^4 square-net layers that were separated by nonmagnetic Al-Ge spacers. MnAlGe exhibits a metallic state with both spin-up and spin-down states with dominant contributions from Mn- d orbitals near the Fermi level (Fig. 4b). 2D arrays of Mn atoms control the electrical, magnetic, and therefore topological properties in MnAlGe. The unique 2D distribution of the Berry curvature resembles the 2D Fermi surface of the bands that formed the topological nodal line near the Fermi energy (Fig. 4c). The ARPES-measured electronic structure agrees well with the first principle calculations with the exception of a slight down-shift of the nodal line energy (Fig. 4d). Within the energy resolution of the experiment, we determined the band crossing point to be approximately 46 ± 18 meV below E_F . The intense surface state that extended to the nodal point further confirmed the topological origin of the band crossing [5].

Transport measurements. MnAlGe exhibits a strong, anisotropic anomalous Hall response. The Hall resistivity, when the magnetic field ($\mu_0 H$) is parallel to the ab -plane, exhibits linear behavior without any saturation (Fig. 5a). When $\mu_0 H$ was applied along the c -axis, the Hall resistivity increased rapidly in the low

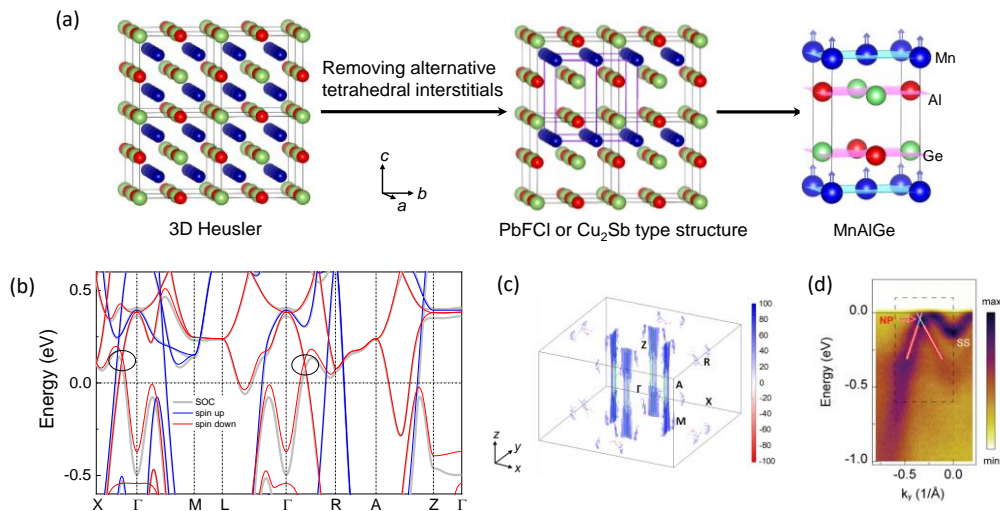


Fig. 4: (a) Representation of the evolution of 3D Heusler arrangement to a layered structure by removal of alternate tetrahedral interstitials. (b) Berry curvature distribution calculated with the inclusion of spin-orbit coupling in the BZ. (c) Band dispersion along Γ -X measured by ARPES with 60 eV photon at 14 K. The red arrow marks the band crossing NP. The very intense electron pocket centered around the Γ -point is a surface state.

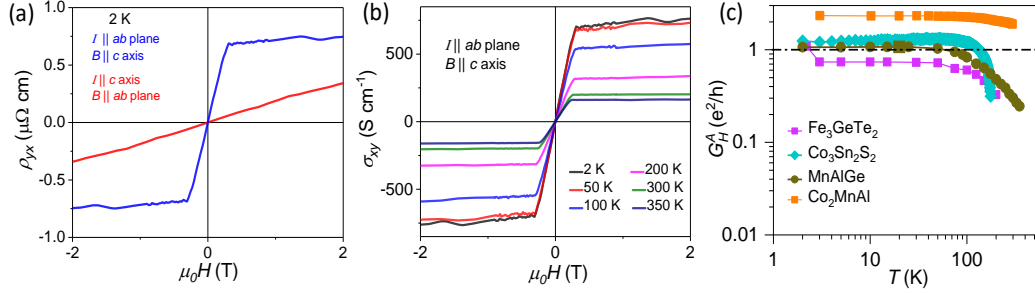


Fig. 5: (a) Magnetic field dependence of the Hall resistivity (ρ_{yx}) with the current within the ab -plane and c -axis of the crystal. (b) Hall conductivity (σ_{xy}) and (c) T -dependence of AHC per magnetic layer for Fe_3GeTe_2 , Co_2MnAl , $\text{Co}_3\text{Sn}_2\text{S}_2$, and MnAlGe .

$\mu_0 H$ regime followed by saturation upon further increase in the $\mu_0 H$. We measured a large AHC value of $\sim 700 \text{ S cm}^{-1}$ at 2 K that is related to nodal line-induced 2D Berry curvature distribution (Fig. 5b). As the AHE in MnAlGe resulted from the 2D band, we estimated the anomalous Hall conductance per ferromagnetic Mn-layer (G_H^A) by multiplying the bulk AHC by the separation between the two Mn-layers. The value of G_H^A at 2 K was $4.153 \times 10^{-5} \text{ S}$, which was close to the quantum conductance for a single electron channel of $\frac{e^2}{h}$ ($3.874 \times 10^{-5} \text{ S}$). For comparison, we also estimated this value for the layered compounds $\text{Co}_3\text{Sn}_2\text{S}_2$ and Fe_3GeTe_2 , as shown in Fig. 5c. The high transition temperature, large anisotropic out-of-plane magnetism, and natural hetero-structure-type atomic arrangements consisting of magnetic Mn and non-magnetic Al/Ge elements render nodal-line MnAlGe as one of the few, unique, and layered topological ferromagnets that have ever been observed [5].

Outlook

Despite extensive active research on topologies, only the tip of the iceberg has been uncovered. A recent theoretical study concludes that $\sim 20\%$ of all the known inorganic compounds are topological. Among the different classes of materials, Heusler compounds are remarkable, more than 1500 in number, which provide an excellent platform for topological research. Recently we investigated intrinsic anomalous transport for all stable magnetic cubic Heusler compounds and found that several of them exhibit very large AHE and ANE [6].

For transport measurements, synthesis of high-quality crystals of the predicted material is essential. We are working on this aspect and recently established that low-cost Fe-based Heusler compounds, Fe_2YZ ($Y = \text{Co, Ni}$; $Z = \text{Al, Ga}$), exhibit a large AHE value in the range of $\sim 250\text{--}750 \text{ S cm}^{-1}$ and a large ANE value of $\sim 2 \mu\text{V K}^{-1}$ near room temperature [7]. Generally, the

Nernst effect is significant when the Fermi level is located near the Weyl or Dirac crossing point. Therefore, isovalent or aliovalent chemical doping could be an excellent strategy to optimize the Nernst signal. Moreover, important points for the material choice are as follows. (a) The Curie temperature should be high, so that a large signal can be achieved close to room temperature or high temperature. (b) The magnetic moment of the compound should be low, to avoid stray fields in the device. (c) Hard magnets are better than soft magnets for zero field signal. We will focus on the synthesis and AHE and ANE properties of materials by using such guidelines and predictions.

This year, we shall set up a new system for high-temperature Nernst measurements. This will extend our flexibility and capacity for measurement of high-temperature thermal transport for topological systems such as those of Co_2MnGa , Co_2MnAl , Fe_3Ga , and Fe_3Al . In future, we shall also investigate various exotic layered magnetic topological materials for observation of quantum anomalous Hall effect and quantum anomalous Nernst effect.

External Cooperation Partners

M. Zahid Hasan, (Princeton University, USA);
A. Damascelli (University of British Columbia Vancouver, BC V6T 1Z4, Canada).

References

- [1]* *Topological quantum materials from the viewpoint of chemistry*, N. Kumar, S. N. Guin, K. Manna, C. Shekhar, and C. Felser, *Chem. Rev.* **121** (2021) 2780.
- [2]* *Discovery of topological Weyl fermion lines and drumhead surface states in a room temperature magnet*, I. Belopolski, K. Manna, D. S. Sanchez, G. Chang, B. Ernst, J. Yin, S. S. Zhang, T. Cochran, N. Shumiya, H. Zheng, et al., *Science* **365** (2019) 1278.
- [3] *Berry curvature and the anomalous Hall effect in Heusler compounds*, J. Kübler and C. Felser, *Phys. Rev. B* **85** (2012) 012405.

- [4]* *Anomalous Nernst effect beyond the magnetization scaling relation in the ferromagnetic Heusler compound Co_2MnGa* , S. N. Guin, K. Manna, J. Noky, S. J. Watzman, C. Fu, N. Kumar, W. Schnelle, C. Shekhar, Y. Sun, J. Gooth, and C. Felser, *NPG Asia Mater.* **11** (2019) 16.
- [5]* *2D-Berry-curvature-driven large anomalous Hall effect in layered topological nodal-line MnAlGe* , S. N. Guin, Q. Xu, N. Kumar, H.-H. Kung, S. Dufresne, C. Le, P. Vir, M. Michiardi, T. Pedersen, S. Gorovikov, et al., *Adv. Mater.* **33** (2021) 2006301, doi.org/10.1002/adma.202006301
- [6]* *Giant anomalous Hall and Nernst effect in magnetic cubic Heusler compounds*, J. Noky, Y. Zhang, J. Gooth, C. Felser, Y. Sun, *NPJ Comput. Mater.* **6** (2020) 77.
- [7] *Large Anomalous Hall and Nernst effects in High Curie-Temperature Iron-Based Heusler Compounds*, F. Mende, J. Noky, S. N. Guin, G. H. Fecher, K. Manna, P. Adler, W. Schnelle, Y. Sun, C. Fu, C. Felser, *Adv. Sci.* (2021) 2100782, doi.org/10.1002/advs.202100782

satyanarayanguin@cpfs.mpg.de